Single-Molecule Magnets

DOI: 10.1002/anie.201202497

A High Anisotropy Barrier in a Sulfur-Bridged Organodysprosium Single-Molecule Magnet**

Floriana Tuna, Charlene A. Smith, Michael Bodensteiner, Liviu Ungur, Liviu F. Chibotaru, Eric J. L. McInnes, Richard E. P. Winpenny, David Collison, and Richard A. Layfield**

Dedicated to Professor Dieter Fenske on the occasion of his 70th birthday

Following the discovery in the early 1990s that individual molecules can exhibit slow relaxation of magnetization and magnetic hysteresis,[1] studies of single-molecule magnets (SMMs) have been dominated by large-spin, exchange-coupled cages of 3d transition metals.[2] In addition to the intrinsic interest in the physics of SMMs, such compounds have been proposed for applications in molecular spintronics and in quantum computing.[3] However, a major obstacle to realizing the applications of SMMs is that energy barriers to magnetization reversal, U_{eff}, and blocking temperatures, T_B, lead to slow relaxation of magnetization only at liquid helium temperatures.

In recent years, there has been a growing realization that focusing on enhancements in magnetic anisotropy rather than on ever-larger spins may be a more effective strategy for increasing U_{eff} and T_B. Therefore, there has been a rise to prominence of the f elements in SMM studies,[4] and lanthanide-containing SMMs (Ln-SMMs) in particular have enabled many exciting developments. For example, in 2003 Ishikawa et al. reported that slow relaxation of magnetization is possible in molecules that contain a single lanthanide ion, namely the terbium(III) phthalocyanine sandwich complex $[\mathrm{TbPc_2}]^-$, with $U_{\mathrm{eff}} = 230\ \mathrm{cm^{-1}}$.[5] The family of lanthanide single-ion magnets (SIMs) continues to grow,[6] and indeed the terbium(III) SIM $[\mathrm{Tb}^i\mathrm{Pc}_2]$ (^{i}Pc = isopropylidenedioxyphthalocyanine), has the highest anisotropy barrier of $U_{\mathrm{eff}} = 556\ \mathrm{cm^{-1}}$.[6e]

Many polymetallic Ln-SMMs, the majority based on dysprosium(III), have also been reported, some of which show impressive SMM properties, such as high values of U_{eff} and/or T_B.[7] The dilanthanide SMMs $[\mathrm{Ln_2\{N(SiMe_3)_2\}_4(thf)_2(\mu{:}\eta^2{:}\eta^2\text{-}N_2)}]^-$ with Ln = Dy or Tb, reported by Evans, Long et al., are arguably the most notable recent examples because the $\mathrm{Ln^{III}}$ ions are strongly exchange-coupled by the radical $[\mathrm{N_2}]^{3-}$ ligand.[8] In the case of the terbium derivative, hysteresis loops in the magnetization versus field plots were observed up to 14 K.

In the majority of Ln-SMMs, the $\mathrm{Ln^{III}}$ ions reside in environments that consist of hard oxygen or nitrogen donor ligands. Whereas the spin configurations of $\mathrm{Ln^{III}}$ ions are insensitive to their environment, their overall electronic structure may be very sensitive. We reasoned that using less-conventional ligands (in the context of SMMs) could be a route to modifying their properties. For example, using soft donors could have two effects: first, magnetic exhange between $\mathrm{Ln^{III}}$ ions could be enhanced; second, very different crystals fields could be generated. Thus, as crystal field effects are the main interactions that lead to slowly relaxing magnetization in Ln-SMMs, there is merit in exploring soft ligand environments. We now report the $\{\mathrm{Dy_2}\}$ SMM $[\{\mathrm{Cp'_2Dy(\mu\text{-}SSiPh_3)}\}_2]$ (**2**, Cp′ = η^5-$\mathrm{C_5H_4Me}$), in which the Dy ions are bridged by thiolate ligands. Compound **2** is the first sulfur-bridged SMM, and the magnetization reversal barrier is the highest yet reported for a $\{\mathrm{Dy_2}\}$ SMM. Ab initio calculations on **2** and related compounds provide insight into the factors that influence the magnetization reversal barrier.

The sulfur-bridged dimers $[\{\mathrm{Cp'_2Ln(\mu\text{-}SSiPh_3)}\}_2]$ (Ln = Gd (**1**), Dy (**2**)) were synthesized by the ligand substitution reactions of $\mathrm{Cp'_3Ln}$ with lithium triphenylsilylthiolate (Scheme 1).

The centrosymmetric dimers crystallize as **1**·(toluene) and **2**·(toluene), and are isostructural (Figure 1; Supporting Information, Figures S1,S2 and Tables S1,S2).

Each $\mathrm{Ln^{III}}$ ion in **1** and **2** is complexed by two η^5-Cp′ ligands and by the sulfur atoms of two μ-$\mathrm{SSiPh_3}$ ligands,

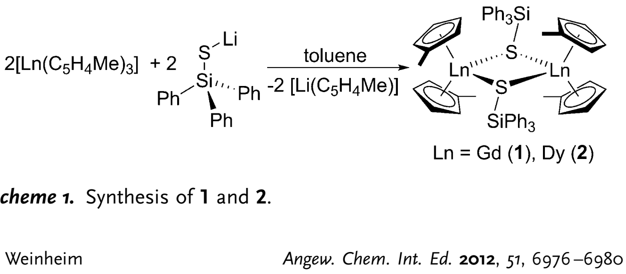

Scheme 1. Synthesis of **1** and **2**.

---

[*] Dr. F. Tuna, C. A. Smith, Prof. E. J. L. McInnes, Prof. R. E. P. Winpenny, Prof. D. Collison, Dr. R. A. Layfield
School of Chemistry and EPSRC UK National EPR Facility
The University of Manchester
Oxford Road, Manchester, M13 9PL (UK)
E-mail: richard.layfield@manchester.ac.uk
Dr. M. Bodensteiner
Institute of Inorganic Chemistry, University of Regensburg
93040 Regensburg (Germany)
Dr. L. Ungur, Prof. L. F. Chibotaru
Division of Quantum and Physical Chemistry
Katholieke Universiteit Leuven
Celestijenlaan 200F, 3001 Leuven (Belgium)

[**] R.A.L. thanks the Alexander von Humboldt Foundation (Fellowship for Experienced Researchers). The EPSRC (UK) are acknowledged. R.E.P.W. thanks The Royal Society for a Wolfson Merit Award. L.U. thanks the FWO-Vlaanderen (Flemish Science Foundation) for a post-doctoral fellowship.

Supporting information for this article is available on the WWW under http://dx.doi.org/10.1002/anie.201202497.

resulting in formal coordination numbers of eight. Alternatively, with respect to Cp ligand centroids and the sulfur atoms, the Dy^{III} centers reside in pseudo tetrahedral geometries, with local C_2 symmetry at Ln (see Table 1 for bond lengths and angles). The asymmetric η^5-Cp coordination mode is reflected in the range of Ln–C distances, which are 2.622(7)–2.707(14) for **1** and 2.599(15)–2.693(10) Å for **2**. The Ln1–S1 and Ln1–S1A distances of 2.7755(14) and 2.7961(15) Å in **1** and 2.7500(15) and 2.7761(16) Å in **2**, combined with the Ln1-S1-Ln1A angles of 101.53(5) and 101.43(6) in **1** and **2**, respectively, show that the Ln_2S_2 rings are rhomboidal. The Ln–C and Ln–S bond lengths and angles in **1** and **2** are typical of compounds of the type $[\{Cp_2Ln(\mu\text{-}SR)\}_2]$ with Ln = Gd or Dy.[9]

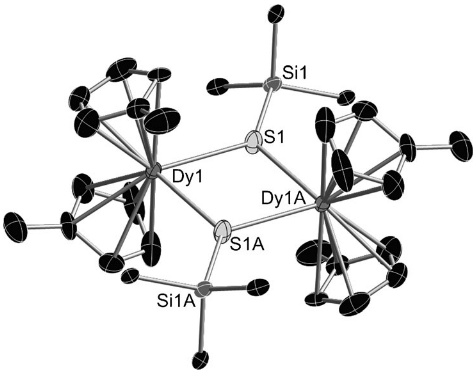

Figure 1. ORTEP representation (ellipsoids set at 50% probability) of the molecular structure of **2**. For clarity, only the *ipso* carbons of the phenyl rings are shown, and the hydrogen atoms are omitted.

Table 1: Selected bond lengths [Å] and angles [°] for **1** and **2**.

	1 (Ln = Gd)	**2** (Ln = Dy)
Ln–C	2.622(7)–2.707(14)	2.599(15)–2.693(10)
Ln1–S1	2.7755(14)	2.7500(15)
Ln1–S1A	2.7961(15)	2.7761(16)
S1-Ln1-S1A	78.47(4)	78.57(5)
Ln1-S1-Ln1A	101.53(5)	101.43(6)

Lanthanide chalcogenolate complexes have been extensively studied because of their applications in organic synthesis and in the catalytic ring-opening polymerization of ε-caprolactone.[10] However, the dynamic magnetic properties of such compounds have not, to the best of our knowledge, been studied previously.

Direct current (dc) magnetic susceptibility measurements on polycrystalline samples of **1** and **2** were carried out in the temperature range 2–300 K in an applied field of 1 kG. For **1**, the value of $\chi_M T$ (χ_M is the molar magnetic susceptibility) per Gd^{III} at 300 K is 15.5 cm^3 K mol^{-1} (Supporting Information, Figure S3), which is in good agreement with the predicted value of $\chi_M T = 15.76$ cm^3 K mol^{-1} for two non-interacting Gd^{III} free ions ($^8S_{7/2}$ ground term, $g = 2$). On cooling, the value of $\chi_M T$ decreases very slowly until about 30 K, and then below 30 K $\chi_M T$ decreases rapidly to reach a value of 6.7 cm^3 K mol^{-1} at 2 K. The absence of first-order spin–orbit coupling in Gd^{III} enables the exchange coupling constant, J, for **1** to be readily determined. Fitting the susceptibility data for **1** using the isotropic spin Hamiltonian $H = -2J[S_{Gd1}\cdot S_{Gd1A}]$, where S_{Gd1} and S_{Gd1A} denote the spins on Gd1 and Gd1A, respectively, produced an excellent fit for $J = -0.105$ cm^{-1}. The same parameters also reproduced the field dependence of the isothermal magnetization of **1** measured at several temperatures between 2–9 K (Supporting Information, Figure S4). These data indicate that the Gd^{III} ions in **1** are weakly antiferromagnetically coupled by the μ-thiolate ligands, which is consistent with other exchange-coupled gadolinium compounds, and can be rationalized in terms of the core-like nature of their valence 4f orbitals.[11]

In **2**, the value of $\chi_M T$ at 300 K is 27.9 cm^3 K mol^{-1}, which agrees well with the expected value of 28.34 cm^3 K mol^{-1} for two magnetically noninteracting Dy^{III} ions with a $^6H_{15/2}$ ground term ($g = 4/3$; Supporting Information, Figure S5). On lowering the temperature, $\chi_M T$ decreases gradually until about 70 K, and then more rapidly to reach 11.2 cm^3 K mol^{-1} at 2 K; this decrease is likely to be due to depopulation of excited m_J sublevels and/or weak antiferromagnetic exchange. At low temperatures, the isothermal $M(H)$ data of **2** are far from reaching saturation under magnetic fields of 0–7 T, and the corresponding $M(H/T)$ curves do not superimpose (Supporting Information, Figure S6), indicating the presence of significant magnetic anisotropy and/or low-lying excited states. The value of the magnetization at 7 T and 1.8 K is 11.4 μ_B (5.7 per Dy^{III} ion), and is similar to that observed in other Dy complexes.[7]

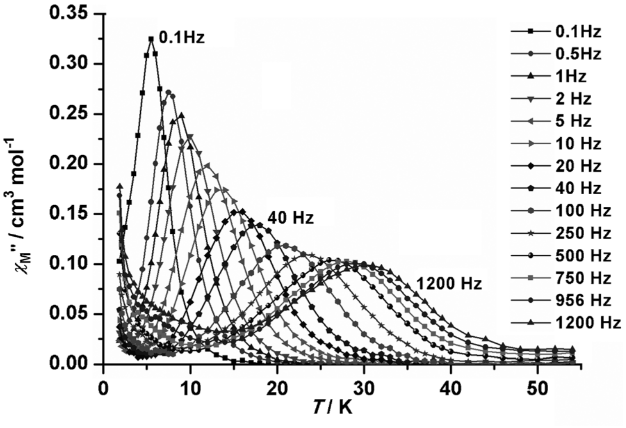

Figure 2. Temperature dependence of χ'' in **2** at various frequencies in zero applied dc field and an ac field of $H_{ac} = 1.55$ Oe.

Both the temperature dependence (Figure 2; Supporting Information, Figure S7) and the frequency dependence (Supporting Information, Figure S8) of the alternating current (ac) susceptibilities of **2** reveal features characteristic of an SMM. In zero dc field, the in-phase (χ') (Supporting Information, Figure S7) and the out-of-phase (χ'') components (Supporting Information, Figure 2) of the ac susceptibility show a frequency dependence up to about 40 K, and a single $\chi''(T,\nu)$ peak is observed below 32 K. Semicircular Cole–Cole plots of χ'' vs. χ' at several temperatures below 32 K were obtained

(Supporting Information, Figure S9), and were fitted by a generalized Debye model using α parameters in the range $\alpha = 0.01$–0.15. This indicates a narrow range of magnetization relaxation times in **2**. Above 20 K, the relaxation in **2** is thermally activated and the Arrhenius plot of $\ln\tau$ versus $1/T$, where τ is the relaxation time constant, is linear (Figure 3).

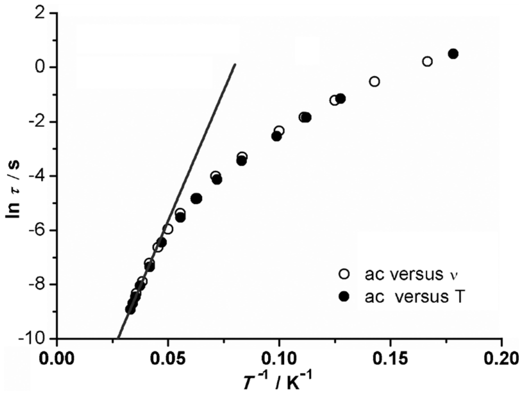

Figure 3. Arrhenius plot of ln τ versus $(1/T)$ for **2**. The solid line is the best fit of the data in the thermally activated regime ($T > 20$ K).

Fitting the higher-temperature data to the Arrhenius law $\tau = \tau_0 \exp(U_{\mathrm{eff}}/k_{\mathrm{B}}\mathrm{T})$ produced an effective energy barrier to magnetization reversal of $U_{\mathrm{eff}} = (133 \pm 3.5)\ \mathrm{cm}^{-1}$ (or (192 ± 5) K) and a pre-exponential factor of $\tau_0 = 2.38 \times 10^{-7}$ s. The SMM behavior of **2** was confirmed by the observation of a narrow hysteresis in magnetization versus field measurements on polycrystalline samples at 1.8 K (Supporting Information, Figure S10).

Compound **2** is the first sulfur-bridged SMM. Organometallic compounds are an interesting alternative chemical repertoire for developing SMMs with unusual physics and high magnetization reversal barriers. Notable recent SMMs based on the dianionic cyclooctatetraene ligand (C_8H_8, COT) include: $[\mathrm{Dy}\{\eta^8\text{-}1,4\text{-}(\mathrm{Me_3Si})_2(\mathrm{COT})\}_2]^-$, which exhibits multiple relaxation modes;[6a] $[(\eta^5\text{-Cp*})\mathrm{Er}(\eta^8\text{-COT})]$;[6b] and neptunocene, $[\mathrm{Np}(\eta^8\text{-COT})_2]$.[6c] The SMMs most closely related to **2** are $[\{\mathrm{Cp_2Dy}(\mu\text{-Cl})\}_n]$ ($n = 2$, **3a**; $n = \infty$, **3b**), $[\mathrm{Cp_2Dy(thf)}(\mu\text{-Cl})]_2$ (**4**) and $[\{\mathrm{Cp_2Dy}(\mu\text{-Bta})\}_2]$ (**5**; Bta = benzotriazolate), which have lower magnetization reversal barriers of $U_{\mathrm{eff}} = 26$, 68, 34, and 33 cm^{-1}, respectively.[12]

Further insight into the magnetization reversal in **2**–**5** was obtained with ab initio calculations,[7b,d,g] using MOLCAS 7.6.[13a] Local magnetic properties on individual Dy ions were computed by the Single_Aniso module,[13b] while the magnetic properties of the dimers were simulated by the Poly_Aniso routine (Supporting Information).[13c] Table 2 shows the energies of the lowest Kramers doublets of the individual Dy ions in **2**–**5**.

Table 2: Energies [cm^{-1}] of the lowest Kramers doublets in **2**–**5**.

No.	**2**	**3a**	**3b**	**4**	**5**
1	0	0	0	0	0
2	113	144	134	96	103
3	283	313	296	193	171
4	368	383	356	211	210
5	386	401	392	236	226
6	426	444	434	286	248
7	457	488	457	308	295
8	624	672	588	339	389

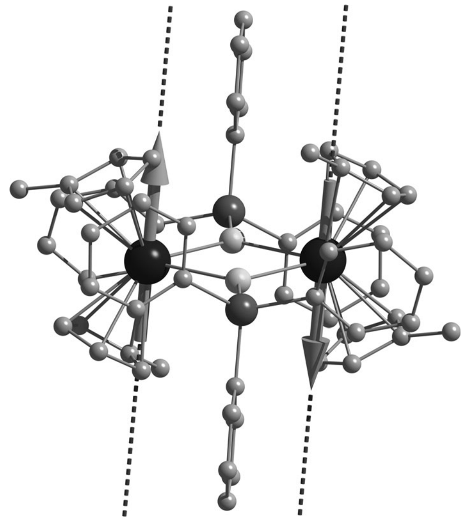

Figure 4. Orientation of the main anisotropy axes (dashed lines) of the ground Kramers doublets of the Dy$^{\mathrm{III}}$ ions (large spheres) in **2**.

Table 3: Principal g values of the ground Kramers doublets in **2**–**5**.

	2	**3a**	**3b**	**4**	**5**
g_x	0.0012	0.0004	0.0009	0.0224	0.0073
g_y	0.0019	0.0009	0.0015	0.0479	0.0884
g_z	19.3611	19.4090	19.3590	18.9208	19.0530

The orientation of the main anisotropy axes of the Dy ions in **2**–**4** is close to perpendicular to the $\{\mathrm{Dy_2X_2}\}$ planes (Figure 4; Supporting Information, Figures S17, S20, S21). The very anisotropic g matrices in the ground doublets (Table 3) mean that the magnetic interaction between Dy ions will be mostly of the Ising type, and so can be described by $\mathrm{H} = -J s_{1z_1} s_{2z_2}$ [Eq. (1)], where s_{1z_1} and s_{2z_2} are projections of the effective spin $\tilde{s} = 1/2$ of lowest Kramers doublets of the two Dy ions on the local anisotropy axes. The magnetic coupling parameter J is a sum of the exchange interaction (J_{exch}) and the magnetic dipole–dipole interaction (J_{dipolar}) between the Dy ions. Knowledge of the ground state g matrix on the Dy sites allows for exact calculations of J_{dipolar} (Table 4), so that the only unknown parameters are J_{exch}, which are derived by fitting the magnetic data (Supporting

Table 4: Dipolar and exchange parts [cm^{-1}] of the magnetic interaction between the Dy$^{\mathrm{III}}$ ions in complexes **2** and **4**.

	2	**4**
J_{exch}	−2.19475	0.08550
J_{dipolar}	−2.22550	−1.99075
$J = J_{\mathrm{exch}} + J_{\mathrm{dipolar}}$	−4.42025	−1.90525

Information, Figures S5, S18, S22). The intramolecular dipolar interaction favors antiferromagnetic coupling between magnetic moments, which is explained by the local anisotropy axes being almost perpendicular to the Dy1⋯Dy2 axis (Figure 4; Supporting Information, Figures S21 for **2** and **4**, respectively). While the dipolar couplings in **2** and **4** are similar, the exchange interaction in **2** is twice as large as that in **4** (Table 4). This is not unexpected, because the valence orbitals of sulfur are more diffuse than those of chloride.

The U_{eff} value of 133 cm^{-1} for **2** agrees well with the calculated energy of the first excited state on Dy sites (113 cm^{-1}). The U_{eff} value of 33 cm^{-1} for thf-solvated **4**, which was extracted in a similar way, does not agree well with the calculated energy of the first excited Kramers doublet (96 cm^{-1}). Analysis of the out-of-phase ac susceptibility of **4** in an applied dc field of 1200 Oe reveals an additional maximum, which is not reached at ac frequencies of less than 1000 Hz and, furthermore, this maximum is not detected in zero applied dc field.[12b] An explanation may be found by considering the two relaxation mechanisms possible in Ln-SMMs: first, a thermally activated (Orbach) mechanism via the first excited state, and; second, a direct mechanism via quantum tunneling of the magnetization (QTM) and/or a Raman process. The rate of the direct process generally correlates with the strength of QTM, and measurements on **4** show that this SMM is in a QTM regime already at $T \approx 5$ K.[12b] A dc field applied to **4** suppresses the QTM and other processes, and on this basis the activated relaxation becomes apparent. In **2**, the QTM and direct relaxation are much less prominent; QTM is not approached even at 2 K and, accordingly, the Orbach process involving the first excited state is measured in the ac susceptibility studies, hence the good match of the energy barriers determined by experiment and by computation.

This interpretation is supported by the calculated values of transverse g values on the Dy ions (g_x and g_y in Table 3), which are one order of magnitude larger in **4** relative to **2**. This implies more prominent QTM (and a larger rate of direct relaxation) in **4**. The same reasoning, based on the "axiality" of the ground Kramers doublet on the Dy sites, explains why the relaxation properties of **5** are similar to those of **4**, whereas the polymeric chains of **3b** behave in a similar manner to **2**. Spurious blocking barriers, which we find here for **4** and **5**, have been encountered in other Ln-SMMs. For instance, the Arrhenius fit of ac susceptibility for $\{\mathrm{Dy}_3\}$ triangles gave a blocking barrier of 25 cm^{-1} in zero dc field, which increased to about 83 cm^{-1} in a dc field of 3 kOe.[7k] The only deviation from this model are the dimeric units of **3a**, which show relatively small transverse g factors on the Dy sites, yet at the same time their magnetization relaxes relatively quickly as in **4** and **5**. The reasons for this inconsistency are currently unclear.

These results illustrate the potential and the complexity of organolanthanide SMMs with soft ligands. Our calculations and most of our observations suggest that the symmetry at the individual Ln sites is crucial in determining the observed U_{eff} value. The transverse g values decide the quantum tunneling rate, and hence whether the complex will fall into an activated or a direct relaxation regime. In low-symmetry cases, with high g factors, it is probable that the direct process is observed.

Received: March 30, 2012
Revised: May 9, 2012

Keywords: ab initio calculations · dysprosium · organometallics · single-molecule magnets · sulfur

---

[1] a) A. Caneschi, D. Gatteschi, R. Sessoli, A. L. Barra, L. C. Brunel, M. Guillot, *J. Am. Chem. Soc.* **1991**, *113*, 5873; b) R. Sessoli, H. L. Tsai, A. R. Schake, S. Y. Wang, J. B. Vincent, K. Folting, D. Gatteschi, G. Christou, D. N. Hendrickson, *J. Am. Chem. Soc.* **1993**, *115*, 1804; c) R. Sessoli, D. Gatteschi, A. Caneschi, M. A. Novak, *Nature* **1993**, *365*, 141.

[2] G. Aromí, E. K. Brechin, *Struct. Bonding (Berlin)* **2006**, *122*, 1.

[3] a) S. Loth, S. Baumann, C. P. Lutz, D. M. Eigler, A. J. Heinrich, *Science* **2012**, *335*, 196; b) M. Mannini, F. Pineider, P. Sainctavit, C. Danieli, E. Otero, C. Sciancalepore, A. M. Talarico, M.-A. Arrio, A. Cornia, D. Gatteschi, R. Sessoli, *Nat. Mater.* **2009**, *8*, 194; c) L. Bogani, W. Wernsdorfer, *Nat. Mater.* **2008**, *7*, 179; d) A. Ardavan, O. Rival, J. J. L. Morton, S. J. Blundell, A. M. Tyryshkin, G. A. Timco, R. E. P. Winpenny, *Phys. Rev. Lett.* **2007**, *98*, 057201; e) M. N. Leuenberger, D. Loss, *Nature* **2001**, *410*, 789.

[4] a) J. D. Rinehart, J. R. Long, *Chem. Sci.* **2011**, *2*, 2078; b) L. Sorace, C. Benelli, D. Gatteschi, *Chem. Soc. Rev.* **2011**, *40*, 3092; c) Y.-N. Guo, G.-F. Xu, Y. Guo, J. Tang, *Dalton Trans.* **2011**, *40*, 9953; d) R. Sessoli, A. K. Powell, *Coord. Chem. Rev.* **2009**, *253*, 2328.

[5] N. Ishikawa, M. Sugita, T. Ishikawa, S. Koshihara, Y. Kaizu, *J. Am. Chem. Soc.* **2003**, *125*, 8694.

[6] a) M. Jeletic, P.-H. Lin, J. J. Le Roy, I. Korobkov, S. I. Gorelsky, M. Murugesu, *J. Am. Chem. Soc.* **2011**, *133*, 19286; b) S.-D. Jiang, B.-W. Wang, H. L. Sun, Z. M. Wang, S. Gao, *J. Am. Chem. Soc.* **2011**, *133*, 4730; c) N. Magnani, C. Apostolidis, A. Morgenstern, E. Colineau, J.-P. Griveau, H. Bolvin, O. Walter, R. Caciuffo, *Angew. Chem.* **2011**, *123*, 1734; *Angew. Chem. Int. Ed.* **2011**, *50*, 1696; d) M. A. AlDamen, J. M. Clemente-Juan, E. Coronado, C. Marti-Gastaldo, A. Gaita-Arino, *J. Am. Chem. Soc.* **2008**, *130*, 8874; e) M. Gonidec, R. Biagi, V. Corradini, F. Moro, V. De Renzi, U. del Pennino, D. Summa, L. Muccioli, C. Zannoni, D. B. Amabilino, J. Veciana, *J. Am. Chem. Soc.* **2011**, *133*, 6603.

[7] a) I. J. Hewitt, J. Tang, N. T. Madhu, C. E. Anson, Y. Lan, J. Luzon, M. Etienne, R. Sessoli, A. K. Powell, *Angew. Chem.* **2010**, *122*, 6496; *Angew. Chem. Int. Ed.* **2010**, *49*, 6352; b) Y.-N. Guo, G.-F. Xu, W. Wernsdorfer, L. Ungur, Y. Guo, J. Tang, H.-J. Zhang, L. F. Chibotaru, A. F. Powell, *J. Am. Chem. Soc.* **2011**, *133*, 11948; c) R. J. Blagg, C. A. Muryn, E. J. L. McInnes, F. Tuna, R. E. P. Winpenny, *Angew. Chem.* **2011**, *123*, 6660; *Angew. Chem. Int. Ed.* **2011**, *50*, 6530; d) P.-H. Lin, T. Burchell, L. Ungur, L. F. Chibotaru, W. Wernsdorfer, M. Murugesu, *Angew. Chem.* **2009**, *121*, 9653; *Angew. Chem. Int. Ed.* **2009**, *48*, 9489; e) Y.-Z. Zheng, Y. Lan, W. Wernsdorfer, C. E. Anson, A. K. Powell, *Chem. Eur. J.* **2009**, *15*, 12566; f) P. H. Lin, T. J. Burchell, R. Clérac, M. Murugesu, *Angew. Chem.* **2008**, *120*, 8980; *Angew. Chem. Int. Ed.* **2008**, *47*, 8848; g) L. F. Chibotaru, L. Ungur, L. Soncini, *Angew. Chem.* **2008**, *120*, 4194; *Angew. Chem. Int. Ed.* **2008**, *47*, 4126; h) C. Aronica, G. Pilet, G. Chastanet, W. Wernsdorfer, J.-F. Jacquot, D. Luneau, *Angew. Chem.* **2006**, *118*, 4775; *Angew. Chem. Int. Ed.* **2006**, *45*, 4659; i) J. Long, F. Habib, P.-H. Lin, I. Korobkov, G. Enright, L. Ungur, W. Wernsdorfer, L. F. Chibotaru, M. Murugesu, *J. Am. Chem. Soc.* **2011**, *133*, 5319; j) J. K. Tang, I. J. Hewitt, N. T. Madhu, G. Chastanet, W. Wernsdorfer, C. E. Anson, C. Benelli, R. Sessoli,

A. K. Powell, *Angew. Chem.* **2006**, *118*, 1761; *Angew. Chem. Int. Ed.* **2006**, *45*, 1729; k) J. Luzon, K. Bernot, I. J. Hewitt, C. E. Anson, A. K. Powell, R. Sessoli, *Phys. Rev. Lett.* **2008**, *100*, 247205; l) J. W. Sharples, Y.-Z. Zheng, F. Tuna, E. J. L. McInnes, D. Collison, *Chem. Commun.* **2011**, *47*, 7650; m) F. Habib, P.-H. Lin, J. Long, I. Korobkov, W. Wernsdorfer, M. Murugesu, *J. Am. Chem. Soc.* **2011**, *133*, 8830.

[8] a) J. D. Rinehart, M. Fang, W. J. Evans, J. R. Long, *J. Am. Chem. Soc.* **2011**, *133*, 14236; b) J. D. Rinehart, M. Fang, W. J. Evans, J. R. Long, *Nat. Chem.* **2011**, *3*, 538.

[9] Cambridge Structural Database, ConQuest software, Version 1.14, accessed March **2012**.

[10] H.-X. Li, Y.-J. Zhu, M.-L. Cheng, Z.-G. Ren, J.-P. Lang, Q. Shen, *Coord. Chem. Rev.* **2006**, *250*, 2059.

[11] a) R. A. Layfield, A. Bashall, M. McPartlin, J. M. Rawson, D. S. Wright, *Dalton Trans.* **2006**, 1660; b) G. Champion, N. Lalioti, V. Tangoulis, M.-A. Arrio, P. Sainctavit, F. Villain, A. Caneschi, D. Gatteschi, C. Giorgetti, F. Baudelet, M. Verdaguer, C. Cartier dit Moulin, *J. Am. Chem. Soc.* **2003**, *125*, 8371.

[12] a) R. A. Layfield, J. J. W. McDouall, S. A. Sulway, F. Tuna, D. Collison, R. E. P. Winpenny, *Chem. Eur. J.* **2010**, *16*, 4442; b) S. A. Sulway, R. A. Layfield, F. Tuna, W. Wernsdorfer, R. E. P. Winpenny, *Chem. Commun.* **2012**, *48*, 1508.

[13] a) F. Aquilante, L. De Vico, N. Ferre, G. Ghigo, P. A. Malmqvist, P. Neogrady, T. B. Pedersen, M. Pitonak, M. Reiher, B. O. Roos, L. Serrano-Andres, M. Urban, V. Veryazov, R. Lindh, *J. Comput. Chem.* **2010**, *31*, 224; b) for SINGLE_ANISO, see: http://www.molcas.org/documentation/manual/node95.html; c) L. Ungur, L. F. Chibotaru, Program POLY_ANISO, University of Leuven, 2006–2012.

[14] a) A. Bhunia, M. T. Gamer, L. Ungur, L. F. Chibotaru, A. K. Powell, Y. Lan, P. W. Roesky, F. Menges, C. Riehn, G. Niedner-Schatteburg, *Inorg. Chem.* **2012**, DOI: 10.1021/ic300065x; b) H. L. C. Feltham, Y. Lan, F. Klöwer, L. Ungur, L. F. Chibotaru, A. K. Powell, S. Brooker, *Chem. Eur. J.* **2011**, *17*, 4362.